Inorg. Chem. **2005**, *44*, 1635–1642

Synthesis, Characterization, and Reactivity of Ti(IV)-Monosubstituted Keggin Polyoxometalates

Oxana A. Kholdeeva,* Tatiana A. Trubitsina, Gennadii M. Maksimov, Anatolii V. Golovin, and Raisa I. Maksimovskaya

Boreskov Institute of Catalysis, Lavrentieva 5, Novosibirsk 630090, Russia

Received July 12, 2004

Ti(IV)-monosubstituted Keggin-type polyoxometalates (Ti-POMs), μ-oxo dimer $[Bu_4N]_8[(PTiW_{11}O_{39})_2O]$ (**1**), and three monomers $[Bu_4N]_4[PTi(L)W_{11}O_{39}]$, where L = OH (**2**), OMe (**3**), and OAr (**4**, ArOH = 2,3,6-trimethylphenol (TMP)), have been prepared starting from μ-hydroxo dimer $[Bu_4N]_7[(PTiW_{11}O_{39})_2OH]$ (**5**) or heteropolyacid $H_5PW_{11}TiO_{40}$ or both. The compounds have been characterized by elemental analysis, IR, UV–vis, and multinuclear (^{31}P, ^{1}H, ^{183}W) NMR. The interaction of **1** and **3**–**5** with H_2O in MeCN produces **2**. The hydrolysis constants, estimated from ^{31}P and ^{1}H NMR data, are 0.006 and 0.04 for **1** and **3**, respectively. Studies by ^{31}P NMR, IR, potentiometric titration, and cyclic voltammetry revealed that **1**–**3** and **5** afford the same protonated titanium peroxo complex $[Bu_4N]_4[HPTi(O_2)W_{11}O_{39}]$ (**I**) upon interaction with aqueous H_2O_2 in MeCN. The rates of formation of **I** correlate with the rates of hydrolysis of the Ti-POMs and follow the order of **5** > **1** > **3**. A two-step mechanism of the reaction of Ti-POMs with H_2O_2, which involves hydrolysis of the Ti–L bonds to yield **2** followed by fast interaction of **2** with hydrogen peroxide producing **I**, is suggested. The equilibrium constant for the reaction of **2** with H_2O_2 to yield **I** and H_2O, estimated using ^{31}P NMR, is 10. The interaction of the Ti-POMs with TMP follows the trends similar to their interaction with H_2O_2 and requires preliminary hydrolysis of the Ti–L bonds. All of the Ti-POMs catalyze the oxidation of TMP with H_2O_2 in MeCN to give 2,3,5-trimethyl-*p*-benzoquinone and 2,2′,3,3′,5,5′-hexamethyl-4,4′-biphenol. The product distribution is similar for all of the Ti-POMs. The catalytic activities of the Ti-POMs correlate with the rates of formation of **I** and follow the order of **2** > **5** > **1** > **3**. The findings lay a basis for a better understanding of the nature of the reactivity of titanium in Ti-catalyzed oxidations.

Introduction

d-Electron transition metal−oxygen−anion clusters, henceforth referred to as polyoxometalates (POMs), are of fundamental and practical interest for people working in different fields of chemistry because of the numerous unique properties of these compounds, such as thermal and hydrolytic stability, tunability of acid and redox properties, solubility in various media, and so forth.[1−10] Because they consist of a close-packed array of oxide anions, they can model discrete fragments of extended metal oxide lattices.[1−6,8,11−13] Ti(IV)-monosubstituted Keggin-type POMs (Ti-POMs) attract our attention as soluble models of titanium centers isolated in an inorganic matrix. It has been well

* Corresponding author. E-mail: khold@catalysis.nsk.su. Fax: (+7)3832309573.

(1) Pope, M. T. *Heteropoly and Isopoly Oxometalates;* Springer: Berlin, 1983.
(2) *Polyoxometalates: From Platonic Solids to Anti-Retroviral Activity;* Pope, M. T., Müller, A., Eds.; Kluwer: Dordrecht, The Netherlands, 1993.
(3) *Polyoxometalate Chemistry: From Topology via Self-Assembly to Applications;* Pope, M. T., Müller, A., Eds.; Kluwer: Dordrecht, The Netherlands, 2001.
(4) Moffat, J. B. *Metal-Oxygen Clusters: The Surface and Catalytic Properties of Heteropoly Oxometalates*; Kluwer/Plenum: New York, 2001.
(5) *Polyoxometalate Molecular Science*; Borrás-Almenar, J. J., Coronado, E., Müller, A., Pope M. T., Eds.; Kluwer: Dordrecht, The Netherlands, 2003.
(6) Pope, M. T. Polyoxo Anions: Synthesis and Structure. In *Comprehensive Coordination Chemistry II*; Wedd, A. G., Ed.; Elsevier Science: New York, 2004; Vol. 4, pp 635−678.
(7) Hill, C. L. Polyoxometalates: Reactivity. In *Comprehensive Coordination Chemistry II*; Wedd, A. G., Ed.; Elsevier Science: New York, 2004; Vol. 4, p 679−759.
(8) Pope, M. T.; Müller, A. *Angew. Chem., Int. Ed. Engl.* **1991**, *30*, 34−48.
(9) Hill, C. L.; Prosser-McCartha, C. M. *Coord. Chem. Rev.* **1995**, *143*, 407−455.
(10) Neumann, R. *Prog. Inorg. Chem.* **1998**, *47*, 317−370.
(11) Day, V. W.; Klemperer, W. G. *Science* **1985**, *228*, 533−541.
(12) Finke, R. G.; Rapko, B.; Saxton, R. J.; Domaille, P. J. *J. Am. Chem. Soc.* **1986**, *108*, 2947−2960.
(13) Chen, Q.; Zubieta, J. *Coord. Chem. Rev.* **1992**, *114*, 107−167.

10.1021/ic0490829 CCC: $30.25
Published on Web 02/10/2005

established that site-isolated titanium species are responsible for the high catalytic activity of Ti-containing microporous and mesoporous materials in the oxidation of a wide variety of organic substrates by aqueous H_2O_2; however, the mechanism of their catalytic action is still under debate.[14−17] Ti-POMs, which are stable toward the hydrolysis of Ti−O−W bonds and oxidative degradation, have been used successfully in several mechanistic studies of a few Ti-catalyzed H_2O_2-based oxidations.[18−22]

Several well-characterized Ti(IV)-monosubstituted POMs have been known, including those having Keggin,[23−28] Dawson,[29−31] and Lindqvist[32] structures. Among Keggin Ti-POMs with P as a central atom, $[PTi(L)W_{11}O_{39}]^{n-}$, those with L = O^{2-},[23] Cp,[24,25] Cl^-, OMe,[26] and O_2^{2-}[27] were reported. Previously, we described the preparation of μ-hydroxo dimer $[Bu_4N]_7[(PTiW_{11}O_{39})_2OH]$ (**5**), and on the basis of the ^{31}P NMR study, we suggested the existence of corresponding μ-oxo dimer $[Bu_4N]_8[(PTiW_{11}O_{39})_2O]$ (**1**) and monomer $[Bu_4N]_4[PTi(OH)W_{11}O_{39}]$ (**2**).[19] Recently, we have reported the synthesis and comprehensive characterization of protonated peroxo complex $[Bu_4N]_4[HPTi(O_2)W_{11}O_{39}]$ (**I**) and its stoichiometric interaction with 2,3,6-trimethylphenol (TMP).[22] Here we present our further progress on the synthesis of the Keggin monosubstituted Ti-POMs and report the preparation of μ-oxo dimer **1** and three monomer derivatives, $[Bu_4N]_4[PTi(L)W_{11}O_{39}]$, where L = OH (**2**), OMe (**3**), and OAr (**4**, ArOH = 2,3,6-trimethylphenol (TMP)), in detail. The interactions of the Ti-POMs with H_2O, H_2O_2, and TMP, which are the key steps in the TMP oxidation with H_2O_2 in the presence of Ti-containing catalysts,[33−35] have been studied. The present work allowed us to gain molecular-level insight into the crucial factors determining the catalytic activity of titanium centers in H_2O_2-based oxidations.

Experimental Section

Materials. Acetonitrile and methanol (Fluka) were dried and stored over 4-Å molecular sieves. Tetra-*n*-butylammonium hydroxide, TBAOH, (1.0 M solution in MeOH, Fluka) was titrated with 1.0 M HCl. H_2O_2 (30 wt % in water) was titrated iodometrically prior to use. TMP was purchased from Fluka and recrystallized from hexane. All of the other reactants were the best available reagent grade and were used without further purification.

Preparations. Heteropolyacid $H_5PW_{11}TiO_{40}\cdot 12H_2O$ was synthesized in a two-chamber electrodialyzer that was described previously.[36,37] Platinized titanium and stainless steel plates (each of $S = 25$ cm^2) were used as the anode and cathode, respectively. The anodic and cathodic chambers (each of $V = 25$ cm^3) were separated by a cation-exchange membrane. The rate of flow in the chambers was 18−20 mL/min; the current density was 0.1 A/cm^2. Two milliliters of titanium(IV) tetrachloride (4 M solution in HCl) was added to 40 mL of an aqueous solution of 0.2 M $Na_7[PW_{11}O_{39}]$.[19] This solution was passed through the anodic chamber of the electrodialyzer. Simultaneously, an aqueous solution of NaOH with an initial concentration of 0.1 M was circulating through the cathodic chamber. Electrodialysis was performed for 5 h. The anolyte solution was steamed to dryness and then kept at 150 °C for 1 h to remove residues of HCl and Cl_2. The resulting white solid was recrystallized from 30 mL of water. Yield: 98%. Anal. Calcd for $H_{29}O_{52}PTiW_{11}$: P, 1.04; Ti, 1.62; W, 68.3. Found: P, 1.01; Ti, 1.61; W, 67.8. IR (1200−400, cm^{-1}) ν: 1070, 1040, 969, 890, 800, 655, 590. ^{31}P NMR (0.2 M in H_2O at 20 °C): $-\delta$ 13.82.[37] ^{183}W NMR (0.2 M in H_2O at 20 °C): $-\delta$ 100.2(2), 100.6(2), 102.7(1), 107.7(2), 118.5(2), 118.9(2).[37] Synthesis of $TBA_7[(PTiW_{11}O_{39})_2OH]$ (**5**) was performed as described earlier (^{31}P NMR in dry MeCN: $-\delta$ 12.76).[19]

$[Bu_4N]_8[(PTiW_{11}O_{39})_2O]$ (1). μ-Oxo dimer **1** was prepared by two different procedures. According to the first procedure, 4 equiv of TBAOH was added to 12.3 g (4.5 mmol) of $H_5PW_{11}TiO_{40}$ dissolved in 20 mL of water. The resulting mixture was vigorously stirred for 5−7 min, and a white precipitate was separated by centrifugation, washed with H_2O, and dried at 70 °C. The resulting solid was dissolved in 15 mL of dry MeCN and after 4 days was precipitated again by adding a 5-fold v/v excess of ether, separated by filtration, washed with ether, and dried at 70 °C. Yield: 9.84 g (80.0%). According to the second procedure, 1 equiv of TBAOH was added to 1.43 g (0.2 mmol) of **5** dissolved in 10 mL of dry MeCN. The resulting mixture was kept over a period of a few hours. Then a white solid was precipitated adding a 5-fold v/v excess of ether, which was filtered off, and the solid was again washed with ether and dried at 70 °C. Yield: 1.29 g (90.2%). To obtain crystals of **1**, 1 equiv of TBAOH was added to 0.09 g of **5** dissolved in 1 mL of dry MeCN. Vapor diffusion of diethyl ether at 4 °C for ca. 2 days resulted in the formation of thin, colorless needles. The number of TBA cations, determined by the ignition of the product at 600 °C, was ca. 8.0. Anal. Calcd for $C_{128}H_{288}N_8O_{79}P_2Ti_2W_{22}$:

(14) Notari, B. *Adv. Catal.* **1996**, *41*, 253−334.
(15) Maschmeyer, T.; Rey, F.; Sankar, G.; Thomas, J. M. *Nature* **1995**, *378*, 159−162.
(16) Corma, A. *Chem. Rev.* **1997**, *97*, 2373−2419.
(17) Clerici, M. G. *Top. Catal.* **2000**, *13*, 373−386.
(18) Kholdeeva, O. A.; Maksimov, G. M.; Maksimovskaya, R. I.; Kovaleva, L. A.; Fedotov, M. A. *React. Kinet. Catal. Lett.* **1999**, *66*, 311−317.
(19) Kholdeeva, O. A.; Maksimov, G. M.; Maksimovskaya, R. I.; Kovaleva, L. A.; Fedotov, M. A.; Grigoriev, V. A.; Hill, C. L. *Inorg. Chem.* **2000**, *39*, 3828−3837.
(20) Kholdeeva, O. A.; Kovaleva, L. A.; Maksimovskaya, R. I.; Maksimov, G. M. *J. Mol. Catal. A: Chem.* **2000**, *158*, 223−229.
(21) Kholdeeva, O. A.; Maksimovskaya, R. I.; Maksimov, G. M.; Kovaleva, L. A. *Kinet. Catal.* **2001**, *42*, 217−222.
(22) Kholdeeva, O. A.; Trubitsina, T. A.; Maksimovskaya, R. I.; Golovin, A. V.; Neiwert, W. A.; Kolesov, B. A.; López, X.; Poblet, J.-M. *Inorg. Chem.* **2004**, *43*, 2284−2292.
(23) Tourné, C. *C. R. Acad. Sci., Ser. C* **1968**, *226*, 702−704.
(24) Ho, R. K. C.; Klemperer, W. G. *J. Am. Chem. Soc.* **1978**, *100*, 6772−6774.
(25) Knoth, W. H. *J. Am. Chem. Soc.* **1979**, *101*, 759−760.
(26) Knoth, W. H.; Domaille, P. J.; Roe, D. C. *Inorg. Chem.* **1983**, *22*, 198−201.
(27) Maksimov, G. M.; Kuznetsova, L. I.; Matveev, K. I.; Maksimovskaya, R. I. *Koord. Khim.* **1985**, *11*, 1353−1356 (in Russian).
(28) Yamase, T.; Ozeki, T.; Motomura, S. *Bull. Chem. Soc. Jpn.* **1992**, *65*, 1453−1459.
(29) Keana, J. F. W.; Ogan, M. D. *J. Am. Chem. Soc.* **1986**, *108*, 7951−7957.
(30) Qu, L.-Y.; Shan, Q.-J.; Gong, J.; Lu, R.-Q.; Wang, D.-R. *J. Chem. Soc., Dalton Trans.* **1997**, 4525−4528.
(31) Kortz, U.; Hamzeh, S. S.; Nasser, N. A. *Chem.—Eur. J.* **2003**, *9*, 2945−2952.
(32) Clegg, W.; Elsegood, M. R. J.; Errington, R. J.; Havelock, J. *J. Chem. Soc., Dalton Trans.* **1996**, 681−690.
(33) Trukhan, N. N.; Romannikov, V. N.; Paukshtis, E. A.; Shmakov, A. N.; Kholdeeva, O. A. *J. Catal.* **2001**, *202*, 110−117.
(34) Kholdeeva, O. A.; Trukhan, N. N.; Vanina, M. P.; Romannikov, V. N.; Parmon, V. N.; Mrowiec-Białoń, J.; Jarzębski, A. B. *Catal. Today* **2002**, *75*, 203−209.
(35) Trukhan, N. N.; Kholdeeva, O. A. *Kinet. Catal.* **2003**, *44*, 347−352.
(36) Kulikova, O. M.; Maksimovskaya, R. I.; Kulikov, S. M.; Kozhevnikov, I. V. *Izv. Akad. Nauk SSSR, Ser. Khim.* **1991**, *8*, 1726−1732.
(37) Maksimov, G. M.; Maksimovskaya, R. I.; Kozhevnikov, I. V. *Zh. Neorg. Khim.* **1992**, *37*, 2279−2286.

C, 20.76; H, 3.92; N, 1.51; O, 17.07; P, 0.84; Ti, 1.30; W, 54.6. Found: C, 20.63; H, 3.94; N, 1.64; P, 0.87; Ti, 1.22; W, 53.6. IR (1200−400, cm^{-1}) ν: 1065, 960, 880, 800, 640, 585, 520, 500. ^{31}P NMR (0.02 M in dry MeCN at 20 °C): δ −13.29 ($\Delta\nu_{1/2} = 2$ Hz). ^{183}W NMR (0.05M in MeCN at 20 °C): $-\delta$ 92.1, 94.6, 95.2, 100.1, 112.2, 113.0, with the approximate intensity ratio of 2:2:1:2:2:2. The real intensities of the ^{183}W NMR signals (on the order of the increase in the negative δ values) were equal to 1.8, 1.6, 1.0, 1.7, 1.7, and 2.0. Potentiometric titration revealed no acid protons.

$[Bu_4N]_4[PTi(OH)W_{11}O_{39}]$ (2). **1** (0.222 g, 0.03 mmol) was dissolved in 1 mL of MeCN. Vapor diffusion of wet acetone at room temperature for ca. 4 days gave colorless prisms of **2**. The first portion of the crystals was filtered off and dried at room temperature. Yield: 0.088 g (39.6%). The number of TBA cations, determined by the ignition of the product at 600 °C, was ca. 4.0. Anal. Calcd for $C_{64}H_{145}N_4O_{40}PTiW_{11}$: C, 20.70; H, 3.94; N, 1.51; O, 17.24; P, 0.83; Ti, 1.29; W, 54.4. Found: C, 20.80; H, 3.96; N, 1.43; P, 0.86; Ti, 1.22; W, 53.4. IR (1200−400, cm^{-1}) ν: 1070, 950, 880, 800, 590, 465. ^{31}P NMR (0.02 M in dry MeCN at 20 °C): δ −13.34 ($\Delta\nu_{1/2} = 2$ Hz). Because **2** is prone to dimerization in dry MeCN, the signal of **1** at −13.29 ppm appeared in the ^{31}P NMR spectrum after a few hours.

$[Bu_4N]_4[PTi(OMe)W_{11}O_{39}]$ (3). TBAOH (1 equiv) was added to 2.86 g (0.4 mmol) of **5** dissolved in 40 mL of MeCN/MeOH (1:1 v/v). The resulting mixture was kept over a period of 4 days. Then, a white solid was precipitated by adding a 5-fold v/v excess of ether, which was filtered off, and the solid was again washed with ether and dried at 70 °C. Yield: 2.63 g (92.0%). The number of TBA cations, determined by the ignition of the product at 600 °C, was ca. 4.0. Anal. Calcd for $C_{65}H_{147}N_4O_{40}PTiW_{11}$: C, 20.95; H, 3.98; N, 1.50; O, 17.18; P, 0.83; Ti, 1.28; W, 54.3. Found: C, 20.84; H, 3.88; N, 1.60; P, 0.86; Ti, 1.23; W, 53.5. IR (1200−400, cm^{-1}) ν: 1065, 960, 880, 800, 620, 590, 510, 490. ^{31}P NMR (0.02 M in dry MeCN at 20 °C): δ −13.27 ($\Delta\nu_{1/2} = 3$ Hz). ^{183}W NMR (0.05 M in MeCN at 20 °C): $-\delta$ 86.8, 94.2, 97.0, 101.6, 109.6, 113.3, with the approximate intensity ratio of 2:2:1:2:2:2. The real intensities of the ^{183}W NMR signals (on the order of the increase in the negative δ values) were equal to 1.3, 1.6, 0.7, 1.5, 2.0, and 1.5. ^1H NMR (0.02 M in dry *d*-MeCN at 20 °C): δ 4.31 (s, 3H, OC*H*$_3$), 3.16 (m, 32H, TBA), 1.65 (m, 32H, TBA), 1.42 (m, 32H, TBA), 0.99 (m, 48H, TBA). Vapor diffusion of diethyl ether at 4 °C to a MeCN/MeOH (1:1 v/v) solution of **3** afforded X-ray quality colorless prismatic crystals (cubic space group *Im*3*m*).

$[Bu_4N]_4[PTi(OAr)W_{11}O_{39}]$ (4). TMP (0.681 g, 5 mmol) was added to 0.741 g (0.1 mmol) of **5** dissolved in 10 mL of dry MeCN. The resulting mixture was kept at room temperature for 3 days. Crystals of **4** were grown upon ether diffusion to the above solution at room temperature for ca. 2 days. The orange crystals were filtered off, washed with MeCN, and dried at room temperature. Yield: 0.445 g (60.0%). The number of TBA cations, determined by the ignition of the product at 600 °C, was ca. 4.0. Anal. Calcd for $C_{73}H_{156}N_4O_{40}PTiW_{11}$: C, 22.89; H, 4.08; N, 1.46; O, 16.71; P, 0.81; Ti, 1.25; W, 52.8. Found: C, 22.61; H, 3.97; N, 1.43; P, 0.83; Ti, 1.23; W, 51.7. IR (1300−400, cm^{-1}) ν: 1270, 1220, 1150, 1065, 955, 880, 800, 610, 590, 515, 495. ^{31}P NMR (0.02 M in dry MeCN at 20 °C): δ −13.18 ($\Delta\nu_{1/2} = 3.5$ Hz). ^{183}W NMR (0.05 M in MeCN at 20 °C): $-\delta$ 89.1, 91.6, 94.5, 98.7, 110.3, with the approximate intensity ratio of 2:2:1:2:4. The real intensities of the ^{183}W NMR signals (on the order of the increase in the negative δ values) were equal to 2.0, 1.9, 1.0, 2.0, and 4.4. ^1H NMR (0.02 M in dry *d*-MeCN at 20 °C): δ 6.84 (d, $J_{HH} = 7.6$ Hz, 1H, TMP), 6.65 (d, $J_{HH} = 7.6$ Hz, 1H, TMP), 3.14 (m, 32H, TBA), 2.40 (s, 3H, TMP), 2.45 (s, 3H, TMP), 2.21 (s, 3H, TMP), 1.64 (m, 32H, TBA), 1.41 (m, 32H, TBA), 0.97 (m, 48H, TBA) (Figure S1 in the Supporting Information (SI)). UV−vis (Figure S2 in the SI): shoulder at 320−350 nm ($\epsilon_{333} = 6990$ $M^{-1}cm^{-1}$). Vapor diffusion of diethyl ether at 4 °C to a dry MeCN solution of **4** afforded X-ray quality yellow prismatic crystals (cubic space group *Im*3*m*). However, in cases **3** and **4**, the structure could not be solved because of the crystal disorder problem.

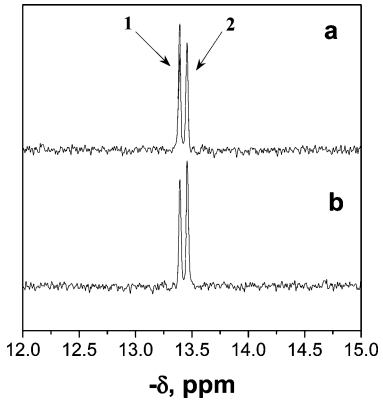

Figure 1. ^{31}P NMR spectra of $[Bu_4N]_8[(PTiW_{11}O_{39})_2O]$ (**1**) and $[Bu_4N]_4[PTi(OH)W_{11}O_{39}]$ (**2**) in equilibrium ([**1**]$_0$ = 0.01 M, MeCN, 7 days): (a) [H_2O] = 2.65 M and (b) [H_2O] = 5.05 M.

Estimation of Equilibrium Constants. Concentrations of the Ti-POMs were estimated from the relative intensities of their ^{31}P NMR signals. The ^{31}P NMR measurement conditions (see Instrumentation and Methods) were adequate for a quantitative (within an error of 10%) determination of the Ti-POM concentrations. The intensity of the ^{31}P signal is proportional to the concentration of a Ti-POM and to the number of P atoms in it. For dimer **1**, which contains two P atoms, the intensity of its ^{31}P NMR signal was divided by two in all of the calculations involving the concentration of **1**. Hydrolysis constants K_1 and K_2 were estimated in MeCN at 22 °C. The value of K_1 was assessed by integrating the ^{31}P NMR signals of **2** and **1** (Figure 1). The value of K_2 was estimated using both ^{31}P NMR and ^1H NMR by integrating signals of **1**−**3** (Figure S3 A in the SI) and by integrating signals of CH_3 protons of **3** and free methanol at 4.31 and 3.25 ppm, respectively (Figure S3 B in the SI). The initial concentration of Ti-POMs was varied in the range of 0.005−0.02 M. The water concentration was varied in the range of 0.55−5.5 M (1−10% v/v). The peroxo-complex formation constant (K_4) was evaluated in MeCN at 22 °C at [**2**] = 0.01−0.02 M and [H_2O_2] = 0.2−0.5 M by integrating ^{31}P NMR signals of **1**, **2**, and **I** (Figure 2). Equilibrium constant K_5 for the reaction of **2** with TMP was estimated at [**2**] = 0.007−0.02 M and [TMP] = 0.2−0.5 M by integrating ^{31}P NMR signals of **2** and **4** (Figure S4 in the SI). Steady values were obtained for all of the equilibrium constants (K) within an error of 20% when concentrations of the Ti-POMs and other reagents were varied in the ranges indicated; no systematic drift was observed.

Interaction of Ti-POMs with H_2O_2. The interaction of Ti-POMs with H_2O_2 was studied in MeCN at 22 °C using both ^{31}P NMR ([Ti-POM] = 0.005−0.01 and [H_2O_2] = 0.15−0.35 M) and UV−vis ([Ti-POM] = 0.0005−0.001 and [H_2O_2] = 0.035 M). In the latter case, concentrations of **I** were calculated using $\epsilon = 1600$ $M^{-1}cm^{-1}$ ($\lambda = 395$ nm), which had been determined previously.[22]

Catalytic Oxidation of TMP. Catalytic oxidations of TMP with H_2O_2 in the presence of Ti-POMs were carried out in temperature-controlled glass vessels at 80 °C, [Ti-POM] = 0.005−0.01, [TMP] = 0.1, and [H_2O_2] = 0.35 M. Biphenyl was added as an internal

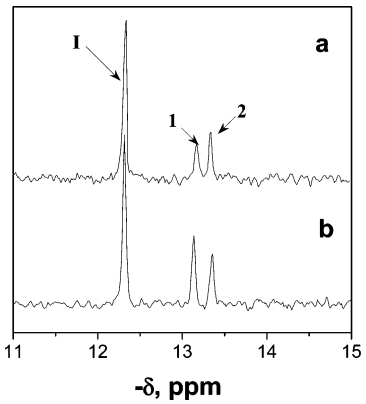

Figure 2. ^{31}P NMR spectra of $[Bu_4N]_4[PTi(OH)W_{11}O_{39}]$ (**2**), $[Bu_4N]_8[(PTiW_{11}O_{39})_2O]$ (**1**), and $[Bu_4N]_4[HPTi(O)_2W_{11}O_{39}]$ (**I**) in equilibrium ($[\mathbf{2}]_0$ = 0.01 M, MeCN, 7 days): (a) $[H_2O_2]$ = 0.2 M and (b) $[H_2O_2]$ = 0.1 M.

standard for GC. Samples were taken during the reaction course and analyzed by GC and GC−MS.

Instrumentation and Methods. The TMP conversion was determined by GC using a Tsvet-500 gas chromatograph equipped with a flame ionization detector and a 25 m × 0.3 mm capillary column filled with carbowax 20 M (Ar, 100−230 °C, 10 °C/min). The oxidation products were identified by GC−MS using a Saturn 2000 gas chromatograph equipped with a CP-3800 mass spectrometer. The ^{183}W NMR spectra (16.67 MHz) of saturated solutions (~0.04 M) of the Ti-POMs in CH_3CN were recorded at room temperature in 10-mm o.d. tubes on an MSL-400 Brüker NMR spectrometer. Typical operation conditions were as follows: sweep width, 2.5 kHz; pulse width, 50 μs (90° flip angle); acquisition time, 1s; and pulse repetition time, 5 s. The number of scans was from 4000 to 12 000 for different samples. Chemical shifts, δ, were referenced to the signal of WO_4^{2-} in a 2 M solution of Na_2WO_4. A saturated solution of $H_4SiW_{12}O_{40}$ (δ −103.65 ppm) was used as a secondary external standard. The ^{31}P NMR spectra of Ti-POMs were measured in MeCN at an operating frequency of 161.98 MHz, with a sweep width of 5 kHz, a pulse width of 10 μs (90° flip angle), and a pulse repetition time of 30 s. Chemical shifts were referenced to 85% H_3PO_4 (external standard). ^{1}H NMR spectra were recorded in *d*-MeCN at 250.13 MHz on a DPX-250 Brüker spectrometer; chemical shifts were referenced to tetramethylsilane. The error in measuring δ was in the range of ±0.05, 0.01, and 0.1 ppm for ^{31}P, ^{1}H, and ^{183}W NMR spectra, respectively. The IR spectra were recorded for 0.5−1.0 wt % samples in KBr on a Specord-75 IR or a Shimadzu FTIR-8300 spectrometer. The electronic absorption spectra were run on a Specord M40 spectrophotometer using 1-cm thermostated quartz cells.

Results and Discussion

Synthesis and Characterization of Ti-POMs. μ-Oxo dimer $[Bu_4N]_8[(PTiW_{11}O_{39})_2O]$ **1** can be obtained either directly from heteropolyacid $H_5PW_{11}TiO_{40}$ or from μ-hydroxo dimer **5**, the preparation and characterization of which has been described previously.[19] In the former case, the heteropolyacid was allowed to react with 4 equiv of methanolic TBAOH in an aqueous solution at room temperature. The resulting white solid dissolved in dry MeCN showed two signals in the ^{31}P NMR spectrum at −13.29 and −13.34 ppm. After storing the compound at room temperature, we found that the intensity of the former signal increased at the expense of the latter one. In a few days, the only species present in the MeCN solution was that with the ^{31}P NMR signal at −13.29 ppm. Bearing in mind the dimerization of $[Bu_4N]_5[PTiOW_{11}O_{39}]$ (**6**) in MeCN upon acidification,[19] we suggested that the peaks at −13.29 and −13.34 ppm belong to μ-oxo dimer **1** and corresponding monomer **2**, respectively, which are present in equilibrium (eq 1) (Figure 1).

$$[Bu_4N]_8[(PTiW_{11}O_{39})_2O] + H_2O \underset{K_{-1}}{\overset{K_1}{\rightleftharpoons}} 2[Bu_4N]_4[PTi(OH)W_{11}O_{39}] \quad (1)$$

Indeed, equilibrium 1 can be shifted left or right by adding activated 4-Å molecular sieves or water, respectively. Note that the addition of water causes a slight shift of all of the ^{31}P signals because of a change in the solution's magnetic susceptibility. Specifically, at 5% (v/v) of water in MeCN, the signals of **1** and **2** move to −13.34 and −13.39 ppm, respectively. Using dry MeCN, we found that it is possible to isolate pure **1** (see Experimental Section). Yet, **1** can also be obtained by adding 1 equiv of methanolic TBAOH to a MeCN solution of **5**. Slow vapor diffusion of diethyl ether to this solution at 4 °C gave thin, colorless needles of **1**.

The addition of 1 equiv of methanolic TBAOH to **5** dissolved in 1:1 (v/v) MeCN/MeOH followed by the addition of excess ether resulted in the precipitation of a white solid. After dissolution in dry MeCN, the compound displayed a ^{31}P NMR signal at −13.27 ppm and a characteristic ^{1}H NMR signal at 4.31 ppm, which can be assigned to methoxyl protons.[26] The ratio of the methoxyl protons to CH_2N protons of TBA cations (multiplet at 3.16 ppm) was 1:10 (theoretical value is 1:11), indicating that one OMe group is bound to the Ti-POM. This allowed us to suggest that we had obtained methoxyl derivative **3**. This compound was first prepared by Knoth in 1983 starting from $[Bu_4N]_4[PTiClW_{11}O_{39}]$ and sodium methoxide.[26] The ^{1}H NMR spectrum of the Knoth methoxyl derivative is identical to that of our compound **3**. Vapor diffusion of diethyl ether at 4 °C to a MeCN/MeOH solution of **3** afforded X-ray quality colorless prismatic crystals. The X-ray single-crystal study confirmed the monomeric Keggin structure of **3**. Unfortunately, the anion was statistically disordered because of the highly symmetric cubic space group (*Im*3*m*), and the position of the TiOMe fragment was therefore impossible to determine. Note that this is a common problem of monosubstituted Keggin M-POMs.[1,22,28]

Our first attempts to obtain pure **2** failed because this species has a tendency to dimerize. Nevertheless, we have found that when **1** was exposed to the vapor diffusion of wet (not specially dried) acetone the first portion of the crystals showed the ^{31}P NMR signal at −13.34 ppm in MeCN. The chemical shift of this signal is similar to those of **1** (−13.29) and **6** (δ −13.32).[19] However, after storing the solution for a few hours, the signal of **1** at −13.29 ppm gradually appeared, whereas the intensity of the resonance at −13.34 ppm decreased simultaneously, indicating the transformation of **2** to **1**. Note that **6**, which has a terminal Ti=O bond, is not prone to dimerization in the absence of

acid.[19] One can see that because the chemical shifts of the ^{31}P NMR signals are close for **1**−**3** and **6** identification of the isolated individual Ti-POMs based only on ^{31}P NMR can be erroneous. Specifically, that could be the reason for some of the contradicting results that have been published in a few papers devoted to catalysis by Ti-POMs.[19,38−41]

Yellow crystals of aryloxy derivative **4** were grown upon slow ether diffusion to a MeCN solution of **5** or **2** in the presence of a 100-fold excess of TMP. Recrystallization from dry MeCN gave pure **4** (^{31}P NMR: δ −13.18 in MeCN). Both the elemental analysis data and the ^{1}H NMR spectrum (see the Experimental Section and SI) of **4** are consistent with a monomer structure of the Ti-POM bearing one TMP ligand bound to Ti. Indeed, if the aryloxy derivative were a μ-OAr dimer, $[Bu_4N]_7[(PTiW_{11}O_{39})_2OAr]$, then the ratio between one of the two aromatic protons of TMP (doublet at 6.84 ppm) and the N−CH_2 protons of TBA (multiplet at 3.14 ppm) would be expected to be 1:56. In fact, the ratio, estimated from the ^{1}H NMR data, was 1:31 (Figure S1 in the SI). This strongly supports the monomeric structure of **4**, for which the theoretical ratio is 1:32. The monomeric structure is also supported by the IR data (vide infra). The X-ray single-crystal study confirmed the monomeric Keggin structure of **4**, but as in the case of **3**, the anion was statistically disordered because of the highly symmetric cubic space group (*Im*3*m*). It is noteworthy that the ^{1}H signals of all three CH_3 groups in **4** (δ 2.45, 2.40, and 2.21) are shifted compared to those of TMP itself (δ 2.26, 2.20, and 2.11), the shifting being more pronounced for the CH_3 groups, which are closer to the O atom. This argues in favor of the formation of the ArO−Ti bond in **4**. The UV−vis spectrum of **4** (Figure S2 in the SI) shows a strong absorption with a shoulder at 320−350 nm ($\epsilon_{333} = 6990$ $M^{-1}cm^{-1}$), which can be attributed to the ArO → Ti ligand-to-metal charge-transfer band.

Importantly, it is easy to distinguish between the dimer and monomer forms of Ti-POMs using IR (Figure 3). The IR spectrum of **1** is similar to the spectrum of **5** and shows a pronounced band at 640 cm^{-1}, which is characteristic of a Ti−O−Ti bond.[19] In our previous work, we found a similar band in the IR spectrum of μ-hydroxo dimer **5**, the dimeric structure of which was confirmed using an FAB-MS technique.[19] Some difference in the positions of the Ti−(OH)−Ti and Ti−O−Ti bands in the IR spectra, 655[19] and 640 cm^{-1}, respectively, is most likely due to the protonation of the Ti−O−Ti bridging oxygen in **5**. At the same time, the IR spectra of **2**−**4** do not display any band in this region (Figure 3), which indicates the monomeric nature of these compounds unambiguously. Thus, the IR data corroborate the implications of the ^{31}P and ^{1}H NMR data. In contrast to monomer **6**, which has a terminal Ti═O bond,[19] and peroxo

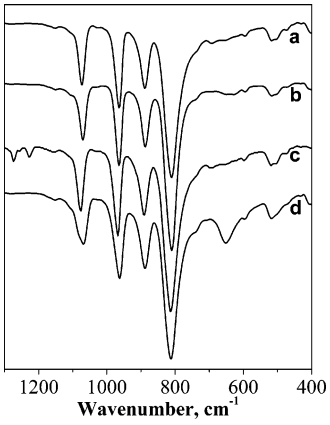

Figure 3. IR spectra of Ti-POMs (1 wt % in KBr): (a) $[Bu_4N]_4[PTi(OH)W_{11}O_{39}]$, (b) $[Bu_4N]_4[PTi(OMe)W_{11}O_{39}]$, (c) $[Bu_4N]_4[PTi(OAr)W_{11}O_{39}]$, and (d) $[Bu_4N]_8[(PTiW_{11}O_{39})_2O]$.

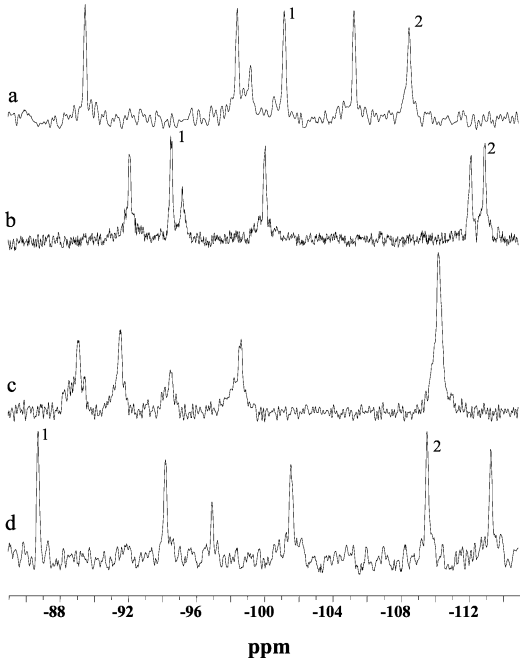

Figure 4. ^{183}W NMR spectra of Ti-POMs (0.04 M in MeCN, 20 °C): (a) $[Bu_4N]_7[(PTiW_{11}O_{39})_2OH]$, (b) $[Bu_4N]_8[(PTiW_{11}O_{39})_2O]$, (c) $[Bu_4N]_4[PTi(OAr)W_{11}O_{39}]$, and (d) $[Bu_4N]_4[PTi(OMe)W_{11}O_{39}]$.

complexes $[Bu_4N]_4H[PTi(O_2)W_{11}O_{39}]$ (**I**) and $[Bu_4N]_5[PTi(O_2)W_{11}O_{39}]$ (**II**),[22] no splitting of the triply degenerate PO_4 stretching mode is observed in the IR spectra of **2**, **3**, and **4** (s 1070, s 1065, and s 1065 cm^{-1}, respectively). This might indicate a higher symmetry around the central PO_4 tetrahedron in **2**−**4** because of a higher formal positive charge of Ti−L with L = OH^-, OMe^{2-}, and OAr^- compared to L = O^{2-} and O_2^{2-}.[42] Interestingly, no splitting of the above-mentioned mode was observed for dimers **1** and **5**. The two additional bands at 1270 and 1220 cm^{-1} that were detected in the IR spectrum of **4** can be assigned to the coordinated TMP molecule.

Figure 4 shows the ^{183}W NMR spectra of **1** and **3**−**5**. It was not possible to record the ^{183}W NMR spectrum of pure **2** in MeCN because **2** dimerized to **1** during the spectrum

(38) Swegler, M.; Floor, M.; Van Bekkum, H. *Tetrahedron Lett.* **1988**, *29*, 823−826.
(39) Kholdeeva, O. A.; Maksimov, G. M.; Fedotov, M. A.; Grigoriev, V. A. *React. Kinet. Catal. Lett.* **1994**, *53*, 331−337.
(40) Yamase, T.; Ishikawa, E.; Asai, Y.; Kanai, S. *J. Mol. Catal. A: Chem.* **1996**, *114*, 237−245.
(41) Kholdeeva, O. A.; Maksimovskaya, R. I.; Maksimov, G. M.; Zamaraev, K. I. *React. Kinet. Catal. Lett.* **1998**, *63*, 95−102.
(42) Rocchiccioli-Deltcheff, C.; Thouvenot, R. *J. Chem. Res. Synth.* **1977**, *2*, 46−47.

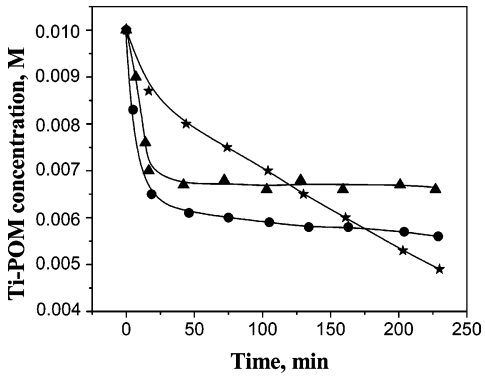

Figure 5. Hydrolysis of Ti-POMs at $[\text{Ti-POM}]_0 = 0.01$ M, H_2O 10% v/v, MeCN, 22 °C: ▲ - $[Bu_4N]_8[(PTiW_{11}O_{39})_2O]$, ★ - $[Bu_4N]_4[PTi(OMe)W_{11}O_{39}]$, and ● - $[Bu_4N]_7[(PTiW_{11}O_{39})_2OH]$.

collecting time. Six lines with an intensity ratio approximately equal to 2:2:1:2:2:2, observed in the ^{183}W NMR spectra of **1**, **3**, and **5**, provide support for the C_s symmetry of these Ti-POMs. The ^{183}W NMR spectrum of **4** (Figure 4c) also indicates C_s symmetry but consists of five (instead of six) peaks because of the overlapping of peaks of two pairs of tungsten atoms. The ^{183}W NMR peaks of **4** are broadened compared to those of the other Ti-POMs that were studied. This broadening may suggest an exchange between some different forms of **4**, for example, Ti−OAr and Ti ← O(H)Ar. Although the ^{31}P NMR chemical shifts are close for some of the Ti-POMs studied, the ^{183}W NMR spectra of all of the Ti-POMs differ markedly in the positions of their six signals. The assignment of the signals to definite tungsten atoms based on the analysis of the ^{183}W−O−^{183}W coupling satellites[26,21,43] is not applicable to spectra with a low signal-to-noise ratio, which is the case for the poorly soluble TBA salts of the Ti-POMs studied in this work. However, an analysis of the relative intensities and heights of the central peaks based on the procedure described in the literature[44] allowed us to assign some of them. According to such an assignment, which agrees with the assignment made using the former approach,[19,26] in the spectrum of **6**, the signal of two tungsten atoms (1) from the same triplet with Ti is significantly shifted to high frequency (−62.4 ppm) as compared with the signal of two other adjacent to Ti tungstens (2) (−112.7 ppm). In the spectrum of **3**, signals (1) and (2) move to −86.7 and −109.6 ppm, respectively (Figure 4d). For **4**, the peaks were not identified because of their broadening and superposition. The δ interval decreases in the order **6** > **3** > **1** ≈ **4** > **5**, which probably reflects a diminution in the heteropolyanion distortion resulting from the replacement of W=O by Ti−L in the Keggin structural unit. This is in agreement with the IR data (vide supra).

Interaction of Ti-POMs with H_2O, H_2O_2, and TMP. The rates of hydrolysis of the Ti-POMs follow the order **5** > **1** ≫ **3** (Figure 5). Although the ^{31}P NMR δ values of the Ti-POMs studied differ insignificantly, the δ difference and the signal sequence are reproducible. Therefore, ^{31}P NMR allows one to distinguish between different Ti-POMs when a few of them are present in equilibrium. Several examples of the ^{31}P NMR spectra of the Ti-POM mixtures are given in Figures 1 and 2 as well as in Figures S3 and S4 in the SI. Because attainment of equilibrium in the Ti-POM mixtures is not fast (several days), one can make a proper assignment of the ^{31}P NMR signals by running spectra immediately after varying initial concentrations of the individual Ti-POMs or several days after introducing the additives (H_2O, MeOH, etc.). Thus, one can see that when H_2O is added to dimer **1** only two species are present in equilibrium: these are dimer **1** and monomer **2** (Figure 1). As we mentioned above, the intensity of the signal of **2** increases with increasing H_2O concentration and decreases upon addition of activated molecular sieves, thus confirming the correctness of eq 1. Hydrolysis constant K_1, calculated from the equilibrium concentrations of **1** and **2** estimated from the corresponding ^{31}P NMR peak intensities, has a value of 6×10^{-3}.

We have studied the hydrolysis of **3** and found that three Ti-POMs, **1**−**3**, can be detected in the equilibrium mixtures by ^{31}P NMR (Figure S3 A in the SI). When a higher excess of H_2O was added, only **1** and **2** were detected. This can be rationalized if we take into account that monomer **2** formed from **3** via eq 2 is prone to dimerization to form **1** (see eq 1). Thus, the general process can be described by eq 3.

$$[Bu_4N]_4[PTi(OMe)W_{11}O_{39}] + H_2O \overset{K_2}{\rightleftharpoons} [Bu_4N]_4[PTi(OH)W_{11}O_{39}] + MeOH \quad (2)$$

$$[Bu_4N]_4[PTi(OMe)W_{11}O_{39}] + [Bu_4N]_4[PTi(OH)W_{11}O_{39}] \overset{K_3}{\rightleftharpoons} [Bu_4N]_8[(PTiW_{11}O_{39})_2O] + MeOH \quad (3)$$

The equilibrium concentrations of **1**−**3** were estimated from the corresponding ^{31}P NMR data (Figure 3S A in the SI), whereas [MeOH] was calculated as $[\mathbf{3}]_0 - [\mathbf{3}]$. The value of K_3 thus assessed was 6. The ratio of [MeOH]/[3] was also determined from the corresponding ^{1}H NMR data (Figure 3S B in the SI), whereas $^{[1]}/_{[2]}$ was assessed from the ^{31}P NMR spectrum (Figure 3S A in the SI). The value of K_3 thus obtained was close to that calculated using the former approach. Using the experimentally obtained values of K_1 and K_3, one can estimate K_2 as $K_3K_1 = 0.04$.

It is well documented that most of the POMs are destroyed by adding excess H_2O_2.[10] Meanwhile, we established previously that the Keggin-type monosubstituted Ti-POMs preserve their structure even when being treated with a 500−1000-fold excess of H_2O_2 in MeCN.[19] In this work, we revealed that all of the Ti-POMs studied, except for **6**,[19,20] produce the same protonated peroxo complex **I** (^{31}P NMR: δ −12.35)[22] upon interaction with H_2O_2. We have reached this conclusion after thorough comparison of the IR, ^{31}P NMR, potentiometric titration, and cyclic voltammetry data for the peroxo complexes isolated from the reaction mixtures after interaction of **1**−**3**, and **5** with a 15-fold molar excess of H_2O_2. The rates of formation of **I** upon interaction with the Ti-POMs with 30% aqueous H_2O_2 decrease in the sequence **2** ≫ **5** > **1** ≫ **3** (Figure 6). In agreement with our

(43) Brevard, C.; Schimpf, R.; Tourne, G.; Tourne, C. M. *J. Am. Chem. Soc.* **1983**, *105*, 7059−7063.
(44) Sveshnikov, N. N.; Pope, M. T. *Inorg. Chem.* **2000**, *39*, 591−594.

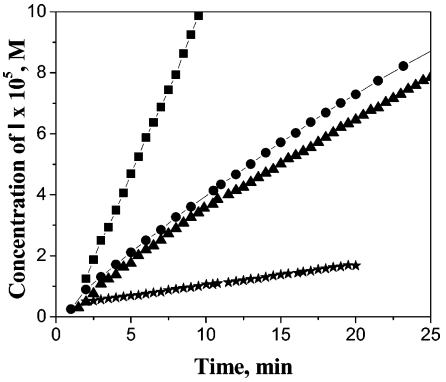

Figure 6. Concentration of $[Bu_4N]_4[HPTi(O_2)W_{11}O_{39}]$ (**I**) versus time upon addition of 30% H_2O_2 (0.035 M) to Ti-POMs (0.001 and 0.0005 M for the monomers and dimers, respectively) in MeCN at 22 °C: ■ - $[Bu_4N]_4[PTi(OH)W_{11}O_{39}]$, ▲ - $[Bu_4N]_8[(PTiW_{11}O_{39})_2O]$, ★ - $[Bu_4N]_4[PTi(OMe)W_{11}O_{39}]$, and ● - $[Bu_4N]_7[(PTiW_{11}O_{39})_2OH]$.

previous data,[20] the rate of peroxo complex formation from the Ti-POMs decreases when concentrated H_2O_2 is used instead of the dilute H_2O_2. All of the facts are consistent with a two-step mechanism of the interaction of Ti-POMs with H_2O_2, which involves hydrolysis to yield **2** (eqs 1 and 2) followed by fast interaction of **2** with hydrogen peroxide to produce **I** (eq 4).

$$[Bu_4N]_4[PTi(OH)W_{11}O_{39}] + H_2O_2 \overset{K_4}{\rightleftharpoons} [Bu_4N]_4[HPTi(O_2)W_{11}O_{39}](\mathbf{I}) + H_2O \quad (4)$$

Equation 4 predicts that adding excess H_2O would shift the equilibrium to the left. The ^{31}P NMR experiments confirm that this is precisely what happens. As in the case of the hydrolysis of **3**, partial dimerization of **2** accompanies reaction 4, which is clearly seen from the ^{31}P NMR data (Figure 2). An estimation of K_4 from the ^{31}P NMR peak intensities gave a value of 10. Importantly, the value of dimerization constant K_{-1} estimated from the spectra given in Figure 2 is close to that assessed independently via eq 1 (Figure 1).

The interaction of the Ti-POMs with TMP in MeCN follows trends similar to their interaction with H_2O_2. First, in the absence of water the reaction is very slow for both **1** and **3**, whereas the addition of ca. 1% H_2O enhances the reaction rate greatly, indicating the requirement of the preliminary hydrolysis of the Ti-POMs to yield **2**. Indeed, **2** reacts easily with excess TMP to give the yellow species showing the ^{31}P NMR resonance at −13.18 ppm. This reaction can be tentatively described by eq 5.

$$[Bu_4N]_4[PTi(OH)W_{11}O_{39}] + ArOH \overset{K_5}{\rightleftharpoons} [Bu_4N]_4[PTi(OAr)W_{11}O_{39}] + H_2O \quad (5)$$

The same species can also be obtained easily from **5** and TMP (see the Experimental Section). Again, protonated dimer **5** is more reactive than its nonprotonated partner **1**. Equilibrium 5 shifts left upon increasing initial concentration of **2** at constant TMP concentration (Figure S4 in the SI) and shifts right upon increasing TMP concentration. The value of K_5, estimated from the ^{31}P NMR data, is 0.03.

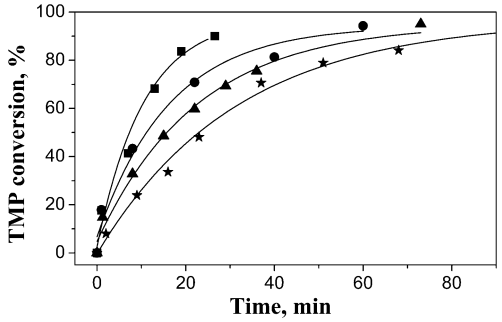

Figure 7. Oxidation of TMP (0.1 M) with 30% H_2O_2 (0.35 M) in MeCN at 80 °C in the presence of Ti-POMs (0.01 and 0.005 M for the monomers and dimers, respectively): ■ - $[Bu_4N]_4[PTi(OH)W_{11}O_{39}]$, ▲ - $[Bu_4N]_8[(PTiW_{11}O_{39})_2O]$, ★ - $[Bu_4N]_4[PTi(OMe)W_{11}O_{39}]$, and ● - $[Bu_4N]_7[(PTiW_{11}O_{39})_2OH]$.

Interestingly, the signal of dimer **1** is not detected in the ^{31}P NMR spectra (Figure S4 in the SI), indicating that excess TMP hampers the dimerization of **2** via eq 1.

Catalytic TMP Oxidation in the Presence of Ti-POMs. We compared the catalytic behavior of the Ti-POMs in the TMP oxidation with H_2O_2 and found that the activity follows the series **2** > **5** > **1** > **3** (Figure 7).As was observed earlier for the thioether oxidation, monomer **6**, which is known to form nonprotonated peroxo complex **II** upon interaction with H_2O_2,[19,20] showed no activity in the catalytic TMP oxidation. The reactivity order found for the Ti-POMs correlates with the rates of peroxo complex formation, which, in turn, correlate with the hydrolysis rates of the corresponding Ti-POMs. The catalytic TMP oxidation in the presence of all of the Ti-POMs yields 2,3,5-trimethyl-*p*-benzoquinone (TMBQ) and 2,2′,3,3′,5,5′-hexamethyl-4,4′-biphenol (BP) as the main reaction products. Recently, we have found the same products for both stoichiometric and catalytic TMP oxidation by peroxo complex **I**.[22] Under the conditions described in the Experimental Section, the yield of TMBQ attained was 30%. For all of the Ti-POMs, the product distribution was similar when the same reaction conditions were employed. However, it depended significantly on the TMP/Ti-POM molar ratio and the reaction temperature in the same way as had been found earlier for the TMP oxidation with H_2O_2 over heterogeneous Ti, Si catalysts.[33−35]

Conclusions

The present work has demonstrated that reliable identification of various forms of Ti-monosubstituted Keggin POMs can be done only by using a combination of multinuclear NMR and IR data. The performed study allowed us to assess the reactivity of different Ti−L bonds, including Ti−OH, Ti═O, Ti−OMe, Ti−OAr, and Ti−O−Ti, toward H_2O, H_2O_2, and TMP and to establish the relationship between this reactivity and the catalytic activity of the Ti-POMs in the TMP oxidation with aqueous H_2O_2. Using the values of K_1−K_5 that were obtained in this work, one can estimate the concentrations of titanium species with different Ti−L bonds in real reaction mixtures, which usually contain a Ti catalyst, H_2O, H_2O_2, MeOH, and an organic substrate. All of these data promote an understanding of the nature of the reactivity of titanium in the Ti-catalyzed oxidations. Detailed

kinetic and mechanistic studies of the alkylphenol Ti-POM-catalyzed oxidation with H_2O_2 will be published in a forthcoming paper.

Acknowledgment. RFBR (grant 04-03-32113) funded the research. We are grateful to K. F. Obzherina for IR measurements. We also thank W. A. Neiwert of Emory University and R. J. Errington of University of Newcastle-upon-Tyne for attempts to perform X-ray structure analysis of the Ti-POMs and C. L. Hill for help and discussion.

Supporting Information Available: ^{1}H and UV−vis spectra for **4**. ^{31}P NMR data for equilibrium mixtures of Ti-POMs. This material is available free of charge via the Internet at http://pubs.acs.org.

IC0490829